Ocean Engineering 64 (2013) 161–173

Contents lists available at SciVerse ScienceDirect

Ocean Engineering

journal homepage: www.elsevier.com/locate/oceaneng

Three-dimensional dynamics of long pipes towed underwater. Part 2 Linear dynamics

M. Kheiri [a], M.P. Païdoussis [a,*], M. Amabili [a], B.I. Epureanu [b]

[a] Department of Mechanical Engineering, McGill University, 817 Sherbrooke Street West, Montreal, QC, Canada H3A 0C3
[b] Department of Mechanical Engineering, University of Michigan, Ann Arbor, MI, USA

ARTICLE INFO

Available online 13 March 2013

Keywords:
Finite difference method
Pinned–pinned pipes
Towed pipes
Divergence
Flutter

ABSTRACT

In this paper, a method of solution based on a finite difference scheme is developed, via which the partial differential equations of motion and boundary conditions, presented in Part 1, are converted into a set of first-order ODEs which are then solved numerically. The mathematical model is validated by considering some simplifications which enable us to compare the numerical results with the results of short pipes simply supported at both ends (pinned–pinned) and subjected to axial flow. A typical Argand diagram is then presented for a long pipe ($\hat{L}=2000$ m) which shows the evolution of lowest three eigenfrequencies of the system as a function of nondimensional flow velocity (towing speed). For the same pipe, the deformation and time-trace diagrams at different values of flow velocity are also given. The results show clearly that a long pipe towed underwater may lose stability by divergence and at higher flow velocities by flutter; the deformation is confined to a small segment of the pipe, close to the downstream end. Some numerical comparisons are also presented in which the effects of cable stiffness and the skin friction coefficient on the onset of instabilities are studied.

1. Introduction

In Part 1 of this two-part study, the equations of motion for the dynamics of long pipes (cylinders) towed underwater have been derived. In fact, these equations can be used to study the dynamics of both long and short pipes subjected to axial flow, since no limiting simplification has been made on the flexural rigidity of the pipe, contrary to some other studies in which, for long pipes, the flexural rigidity of the body has been neglected (e.g., Triantafyllou and Chryssostomidis, 1985) or only partly been taken into account (e.g., Dowling, 1988).

Interest in the dynamics of very slender cylinders, where the length-to-diameter ratio, $\hat{L}/\hat{D}$, is of order 10^2 or even 10^5, subjected to axial flow may also be found in some of the earliest work carried out for possible application to submarine antennas and hydrophone arrays (e.g., Ortloff and Ives, 1969; Pao, 1970; Lee, 1981). In these analyses, which unfortunately were made based on the erroneous version of equations of motion proposed by Païdoussis (1966), and not the corrected ones (Païdoussis, 1973), they found a different stability behaviour for long cylinders from that of short ones.

Recently, in a paper by de Langre et al. (2007), the stability of a thin flexible cylinder subjected to axial flow and fixed at the upstream end has been considered. Contrary to previous predictions made via simplified models (Dowling, 1988; Triantafyllou and Chryssostomidis, 1985), they found that flutter may arise for very long cylinders if the free downstream end of the cylinder is well-streamlined. They also found a limit regime in which the instability characteristics of the system are not affected by the length of the cylinder, and the cylinder deformation is confined to a finite region close to the downstream end.

A number of experiments were conducted (Païdoussis, 1968) with relatively short ($\hat{L}/\hat{D}\simeq 20$) flexible cylinders held in flow by a length of string attached to their upstream end. Later, Ni and Hansen (1978) studied experimentally the flow-induced lateral motions of a flexible tube in axial flow; the flexible tube was very slender ($\hat{L}/\hat{D}\simeq 500$) and approximately neutrally buoyant, and it was fixed at the upstream end and free at the downstream end. A set of experiments were also carried out by Sudarsan et al. (1997) to study the hydroelastic instability of flexible slender cylinders towed underwater. These experiments were conducted in a towing tank, and the models were with length-to-diameter ratios of 50 and 150. Generally, in the above-mentioned experiments divergence and flutter have been observed; moreover, in the case of very slender cylinders, the deformation seems to be centered particularly in the region close to the downstream end of the cylinders.

* Corresponding author. Tel.: +1 514 398 6294; fax: +1 514 398 7365.
E-mail address: michael.paidoussis@mcgill.ca (M.P. Païdoussis).

0029-8018/$ - see front matter © 2013 Elsevier Ltd. All rights reserved.
http://dx.doi.org/10.1016/j.oceaneng.2013.01.007

In this paper, a finite difference scheme is used to spatially discretize the linearized unsteady equations of motion. The resultant set of time-domain ODEs are solved by using DIVPAG routine of Fortran IMSL library. Then, a simplified version of the equations which mimics the dynamical behaviour of short simply supported (pinned–pinned) pipes in axial flow is used to validate the present model. Finally, in the last part of this paper, the numerical results for the dynamics of long pipes flexibly connected to a towing vessel at the upstream end and to a trailing vessel at the downstream end are presented.

It is emphasized that the model considered here, involving long pipes towed underwater and subject to realistic nonclassical boundary conditions, is presented for the first time. In the numerical solutions presented, the effect of various system parameters is examined for the first time. Moreover, this paper presents numerical solutions for both short and long pipes, allowing the reader to understand the dynamical features of both systems, side by side.

2. The method of solution

In this section, the method of solution for the unsteady equations of motion for cases with only axial flow (no cross-current) is discussed. Although equations for both the steady state (related to the effect of a cross-current) and for unsteady self-excited motions have been derived in Part 1, we are not going to present any numerical solutions here for the steady current-induced deformation, since this is not the aim of this study. The dynamics in the presence of a cross-flow is the subject of another paper, currently under preparation.

2.1. The unsteady equations of motion

With no cross-current ($U_z=0$), there is no steady-state deformation in the z-direction. In this case the y- and z-direction equations, as given in Part 1, become identical, and the dynamics of the system can be studied by solving one of them. The equation of motion in the z-direction can be written as

$$\alpha^4\frac{\partial^4 w}{\partial\xi^4}+\alpha^2(U_x^2-\overline{T})\frac{\partial^2 w}{\partial\xi^2}+2\alpha\beta^{1/2}U_x\frac{\partial^2 w}{\partial\xi\partial t}+\frac{1}{2}\alpha U_x^2\varepsilon c_f\frac{\partial w}{\partial\xi}+\left(\frac{1}{2}U_x\varepsilon c_f\beta^{1/2}+\frac{1}{2}\varepsilon c_d\beta^{1/2}\right)\frac{\partial w}{\partial t}+\frac{\partial^2 w}{\partial t^2}=0, \quad (1)$$

in which all quantities are nondimensional. Here w is the displacement in the z-direction, ξ the longitudinal coordinate, and ε a measure of the slenderness ratio defined as $\varepsilon=\hat{\ell}/\hat{D}$ where $\hat{\ell}=[(\pi\hat{D})^2\hat{L}]^{1/3}$; t represents time, and $\hat{L}$ and $\hat{D}$ are the length and the diameter of the pipe, respectively; U_x the axial flow velocity (tow speed), β the ratio of the fluid mass to the total mass (fluid and structure), c_f the frictional drag coefficient, c_d the zero-flow normal coefficient, and α a coefficient used for normalizing the longitudinal coordinate; $\overline{T}$ the steady tension in the pipe, which can be found in the dimensional form in Eq. (17) of Part 1.

The expression for $\overline{T}$ can be written in nondimensional form as

$$\overline{T}=\overline{T}_1-\frac{1}{2\alpha}\varepsilon c_f U_x^2\xi, \quad (2)$$

where $\overline{T}_1$ is the tension at the pipe upstream end. By substituting Eq. (2) into Eq. (1), the equation of motion takes the form

$$\alpha^4\frac{\partial^4 w}{\partial\xi^4}+(c_1\alpha^2+c_2\alpha\xi)\frac{\partial^2 w}{\partial\xi^2}+c_3\alpha\frac{\partial^2 w}{\partial\xi\partial t}+c_4\alpha\frac{\partial w}{\partial\xi}+c_5\frac{\partial w}{\partial t}+\frac{\partial^2 w}{\partial t^2}=0, \quad (3)$$

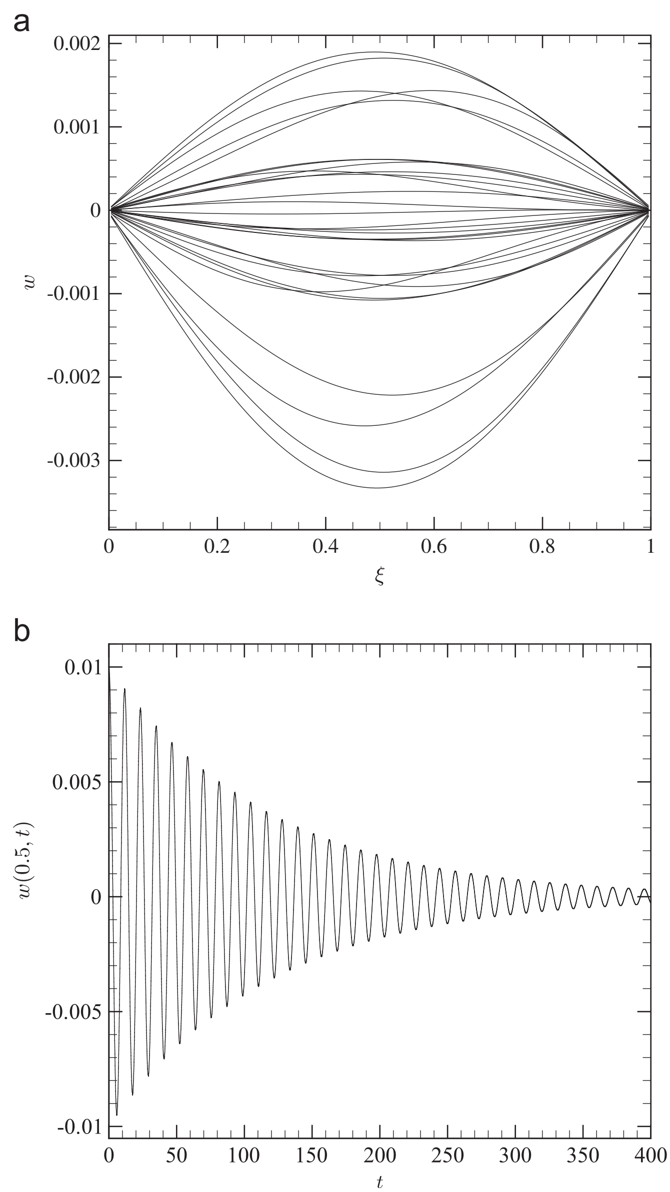

Fig. 2. Typical results showing (a) the shape of a "short pipe" with very stiff end-springs at different time instants and (b) the time trace of the pipe mid-point; $U_x=0.70$.

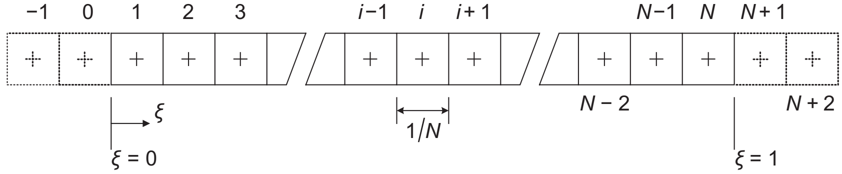

Fig. 1. The spatial discretization: the body is divided into N elements of equal length ($1/N$) with mesh points at the centre of the elements.